Am J Nucl Med Mol Imaging 2024;14(5):337-344
www.ajnmmi.us /ISSN:2160-8407/ajnmmi0157544

Original Article

Normal-organ distribution of PSMA-targeting PET radiopharmaceutical ^{18}F-flotufolastat: a post hoc analysis of the LIGHTHOUSE and SPOTLIGHT studies

Ross Penny[1], Benjamin Fongenie[2], Phillip Davis[3], James Sykes[1]

[1]Blue Earth Diagnostics Ltd., The Oxford Science Park, Magdalen Centre, Robert Robinson Avenue, Oxford, OX4 4GA, UK; [2]Blue Earth Therapeutics Ltd., The Oxford Science Park, Magdalen Centre, Robert Robinson Avenue, Oxford, OX4 4GA, UK; [3]Blue Earth Diagnostics Inc., No. 259 Prospect Plains Road, Building H, Suite 100, Monroe Township, New Jersey 08831, USA

Received May 3, 2024; Accepted July 28, 2024; Epub October 15, 2024; Published October 30, 2024

Abstract: Background: High-affinity radiohybrid PSMA-targeting radiopharmaceutical ^{18}F-flotufolastat (^{18}F-rhPSMA-7.3) is newly approved for diagnostic imaging of prostate cancer. Here, we conduct a post hoc analysis of two phase 3 studies to quantify ^{18}F-flotufolastat uptake in a range of normal organs. Methods: All 718 evaluable ^{18}F-flotufolastat scans from LIGHTHOUSE and SPOTLIGHT were re-evaluated. Additionally, patients' medical records were reviewed and any patients with high tumor burden (PSA>20 ng/mL), altered biodistribution (e.g., chronic kidney disease), major anatomical changes to normal organs (e.g., nephrectomy), or any other history of cancer were excluded. A medical physicist defined volumes of interest over specific organs for evaluation of SUV_{mean} and SUV_{peak} per PERCIST 1.0 criteria. Normally distributed data are reported as mean (SD) and non-normally distributed data as median (IQR). The co-efficient of variation (CoV; calculated as SD/mean for normally distributed data and IQR/median for non-normally distributed data) was used to quantify variability of SUV metrics. Results: In total, scans from 546 patients (244 primary, 302 recurrent) were eligible for this analysis. All organs were considered to be normally distributed except for the bladder and spleen. In the liver, the mean SUV_{mean} was 6.7 (SD 1.7), CoV 26%, while the bladder median SUV_{mean} was 10.6 (IQR 11.9), CoV 112%. The mean SUV_{peak} in the liver was 8.2 (SD 2.1), CoV 26% and median SUV_{peak} in the bladder was 16.0 (IQR 18.5), CoV 116%. Conclusions: Physiological ^{18}F-flotufolastat uptake in normal organs was broadly consistent with other renally-cleared radiopharmaceuticals, which may have clinically significant implications when considering patient selection for radioligand therapy. Additionally, the bladder median SUV_{peak} for ^{18}F-flotufolastat was lower than that previously reported for ^{68}Ga-PSMA-11 and ^{18}F-DCFPyL.

Keywords: Biodistribution, ^{18}F-flotufolastat, liver, positron emission tomography, prostate-specific membrane antigen, rhPSMA

Introduction

Following approval of the first prostate-specific membrane antigen (PSMA) targeting positron emission tomography (PET) radiopharmaceutical by the US Food and Drug Administration (FDA) in 2020 [1], PSMA-PET has become the mainstay for diagnostic imaging in patients with suspected or recurrent prostate cancer, with three radiopharmaceuticals now approved for use in the USA [2-6].

The most recently approved radiopharmaceutical, ^{18}F-flotufolastat (formerly ^{18}F-rhPSMA-7.3), is a high-affinity radiohybrid PSMA-ligand [7]. Data from the Phase 3 LIGHTHOUSE and SPOTLIGHT studies show ^{18}F-flotufolastat to be well tolerated and to provide clinically useful information regarding the presence of N1 and M1 disease prior to surgery in newly diagnosed prostate cancer, and for the localization of recurrent disease, particularly among patients with prostate specific antigen (PSA) levels ≤0.5 ng/mL [8-10]. Moreover, a post hoc analysis of over 700 scans from across the two studies confirmed early clinical data suggesting ^{18}F-flotufolastat has low average urinary excretion and showed that in 96% of patients ^{18}F-flotufolastat image assessment is not impacted by urinary activity (majority read data) [11, 12]. Within professional body guidelines ^{18}F-flotufolastat is considered among a common class of radiopharmaceuticals for PET/computed tomography (CT), collectively referred to as PSMA-ligands or PSMA-PET [2, 13].

Further to the role of PSMA-PET radiopharmaceuticals in diagnostic imaging, the March 2022 approval of ^{177}Lu-PSMA-617 (^{177}Lu-vipivotide tetraxetan) radioligand therapy for patients with metastatic castration resistant prostate cancer (mCRPC) has prompted the additional clinical use of PSMA-PET for the selection of patients with mCRPC who may be suitable for PSMA radioligand therapy (RLT) [2, 14]. Following approval of ^{177}Lu-PSMA-617, the FDA included in the indication for Locametz (kit for preparation of gallium ^{68}Ga-PSMA-11) the selection of patients with mCRPC for whom ^{177}Lu-PSMA-617 directed therapy is indicated [15]. Data from the Vision trial supported approval of Locametz for this indication, where PSMA-positive disease was generally defined as the presence of at least one tumor lesion with ^{68}Ga-PSMA-11 uptake greater than normal liver [15, 16].

Subsequently, the Society of Nuclear Medicine and Molecular Imaging (SNMMI) PSMA PET Appropriate Use Criteria (AUC) Working Group suggested that ^{18}F-DCFPyL

could be considered equivalent to ^{68}Ga-PSMA-11 for ^{177}Lu-PSMA-617 patient selection based on comparable biodistribution data for ^{18}F-DCFPyL and ^{68}Ga-PSMA-11, particularly in the liver, given its common use as a reference organ [4, 5, 14, 17]. To date, only two studies (N=34 and N=11 subjects) of note have been published that compare normal-organ biodistribution of ^{68}Ga-PSMA-11 and ^{18}F-DCFPyL using either absolute SUV metrics or tumor-to-liver ratios [18, 19].

Most recently, following FDA approval of ^{18}F-flotufolastat, the latest National Comprehensive Cancer Network (NCCN) prostate cancer guidelines state that owing to the equivalency of normal-organ distribution of the three FDA-approved PSMA-PET radiopharmaceuticals, ^{18}F-DCFPyL and ^{18}F-flotufolastat may also be used with ^{177}Lu-PSMA-617 [2]. The 2024 SNMMI AUC update also recommends that ^{18}F-flotufolastat can be used for ^{177}Lu-PSMA-617 patient selection but notes there to be limited data on the biodistribution of ^{18}F-flotufolastat and how it compares with ^{18}F-DCFPyL and ^{68}Ga-PSMA-11 [20].

Given the important relationship of normal-organ biodistribution and PSMA-PET interpretation, especially in the liver due to its use as a reference organ for radioligand therapy patient selection, we conducted a post hoc analysis of a large population of patients to quantify the uptake of ^{18}F-flotufolastat in the liver and other normal organs in all evaluable patients who underwent ^{18}F-flotufolastat PET/CT as part of either the LIGHTHOUSE or SPOTLIGHT study.

Materials and methods

Patient population

As previously reported, the Phase 3 LIGHTHOUSE (NCT04186819) and SPOTLIGHT (NCT04186845) studies assessed the diagnostic performance of ^{18}F-flotufolastat in patients with newly diagnosed, unfavorable intermediate to very high-risk prostate cancer, or in patients experiencing biochemical recurrence, respectively [8, 9]. Both studies were performed in line with the principles of the Declaration of Helsinki and approved by the relevant Ethics Committees. All patients provided written informed consent [8, 9].

All 718 evaluable scans from the efficacy populations (352 from the LIGHTHOUSE and 366 from the SPOTLIGHT study) were reviewed for this post hoc analysis. In addition, the medical history data from the original studies were reviewed for each patient and any patients meeting the following criteria were excluded from the present analysis: high tumor burden (defined as baseline PSA>20 ng/mL); altered biodistribution (e.g., chronic kidney disease, hepatic cysts); major anatomical changes in the normal organs under study (e.g., nephrectomy, cystectomy); or any other history of cancer or additional primary cancer.

^{18}F-flotufolastat PET/CT

Patients were asked to continue taking any prescribed medications; to arrive for their appointment well hydrated; and to void immediately prior to entering the scanning room. The target administered activity of ^{18}F-flotufolastat was 296 MBq (median [range] activity 307.3 MBq [213.5-397.8 MBq] in LIGHTHOUSE; 306.0 MBq [230.1-355.2 MBq] in SPOTLIGHT) [8, 9]. At 50-70 minutes post-injection, the PET/CT acquisition was started with a time per bed position of 3 minutes, in a caudal-cranial direction from mid-thigh to skull base. No co-administration of x-ray contrast agent was allowed, and no late imaging was performed. Images were iteratively reconstructed, utilizing time-of-flight if available; no point-spread-function correction algorithms were used. All PET systems in these multisite studies were approved by the image core lab prior to scanning the first patient.

Image analysis

The present post hoc analysis utilized a comparable methodology to Ferreira *et al* to facilitate general comparison of the peak standardized uptake value (SUV_{peak}) for ^{18}F-flotufolastat to those previously reported for ^{68}Ga-PSMA-11 and ^{18}F-DCFPyL [18].

A professionally-accredited medical physicist used image review software (MIM Encore™, version 7.2, MIM Software Inc., Cleveland, USA) to define and outline the volumes of interest (VOIs) over the following organs using either a semi-automated tool (PET Edge®), or spheres: lacrimal glands (20 mm sphere); parotid glands and sub-mandibular glands; lumen of the descending thoracic aorta (20 mm sphere); parenchyma of the right hepatic lobe (60 mm sphere); kidneys; third portion of the duodenum; urinary bladder contents; and gluteal muscle (20 mm sphere), as illustrated in **Figure 1**. In cases where the physiological activity was similar to adjacent local background and the semi-automated tool could not be used, the low dose CT scan was used to define or amend the VOI boundary. The placement of each outline was reviewed by a qualified nuclear medicine physician to ensure accuracy and standardization, as well as to ensure that pathological disease was excluded from the results.

Mean standardized uptake value (SUV_{mean}) and peak standardized uptake value (SUV_{peak}), as defined in the PERCIST 1.0 criteria [21], were computed for each VOI using the native semi-automated tool in the image review software. For paired organs, the arithmetic mean SUV metric is given. In patients where either the lacrimal glands, or both the lacrimal glands and parotid glands were not included in the scan field of view, if all other eligibility criteria were met then it was assumed that biodistribution was not affected, and the SUV metrics for other organs were included in the dataset. In patients where only a single side of the paired organ was visible, the SUV metrics for that organ were excluded.

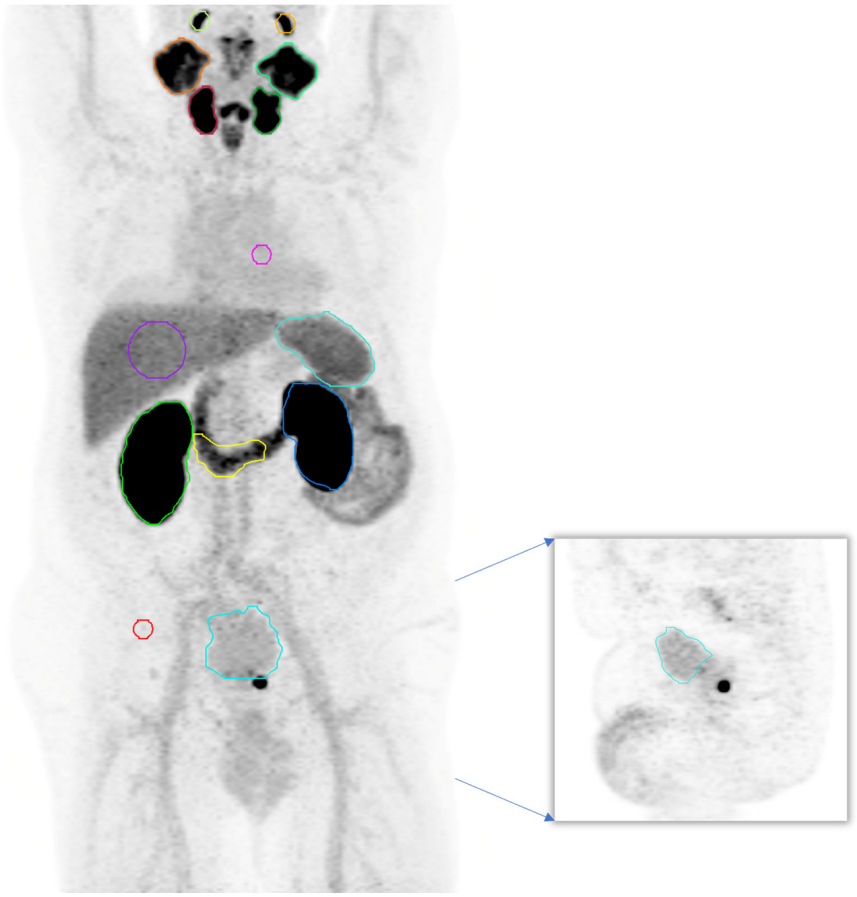

Figure 1. Maximum intensity projection ^{18}F-flotufolastat PET scan of a patient with prostate cancer (SUV scale 0-10). Representative volumes of interest (VOIs) are shown on each of the normal organs measured in this analysis (left). Sagittal image (right lower) showing care was taken to ensure the bladder VOI did not include ^{18}F-flotufolastat avid local disease, also afforded by the comparatively low degree of urinary activity within the bladder in this case.

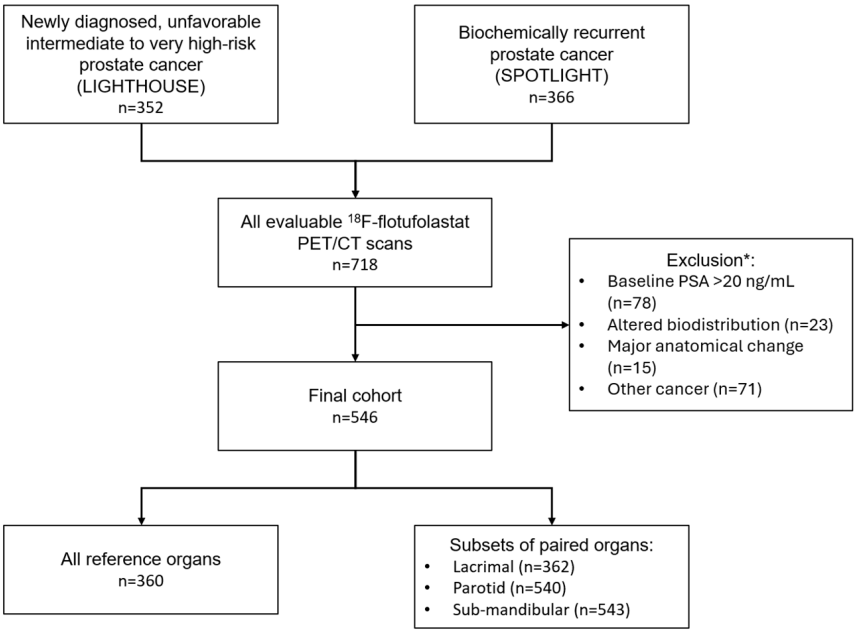

Figure 2. Patient flow chart. *Patients may have met ≥1 exclusion criteria.

This method also builds upon a previously published analysis conducted in the same patient population [11] by extending their assessment of ^{18}F-flotufolastat urinary activity in a single slice over the maximum radioactive bladder diameter to a quantitative assessment of the entire radioactive bladder volume.

Statistics

Statistical analysis was performed using SAS Version 9.4 (SAS Institute Inc., Cary, NC). Violin and box-and-whisker plots were created in R Stats (R Foundation for Statistical Computing, Vienna, Austria). Data were assessed for normality via review of the histogram and Q-Q plots. Shapiro-Wilk, as used in Ferreira *et al* [18], was not used due to the large sample size and the known oversensitivity in large datasets. Normally distributed data are reported as the arithmetic mean and standard deviation (mean (SD)). Non-normally distributed data are presented as the median and interquartile range (median (IQR)). Variability of SUV metrics for each organ was quantified using the co-efficient of variation (CoV), calculated as the SD/mean for normally distributed data and IQR/median for non-normally distributed data.

Results

A total of 718 subjects were available for analysis in this post hoc study (**Figure 2**); of these, 546 (244 primary, 302 recurrent) met the additional eligibility criteria and were included in the final cohort.

For the subset of paired organs at the extreme axial field of view, a total of 362 lacrimal, 540 parotid and 543 sub-mandibular locations were found to be sufficiently within the field of view to be included in the results.

Biodistribution

Quantitative data for all organs are presented in **Table 1**. SUV data for all organs were considered to be normally distributed except for the bladder and spleen. **Figure 3** presents SUV distribution data for the key organs analyzed in this report (liver and bladder).

Table 1. Summaries of SUV_{mean} (A) and SUV_{peak} (B) ^{18}F-flotufolastat physiological activity in normal organs

A. SUV_{mean} physiological activity					
Organ	n	Statistic	SUV_{mean}	SD/IQR	CoV
Aorta	546	Mean	1.9	0.4	22%
Bladder	546	Median	10.6	11.9	112%
Duodenum	546	Mean	7.4	2.5	33%
Gluteal	546	Mean	0.6	0.1	19%
Kidney	546	Mean	22.4	5.5	25%
Lacrimals	362	Mean	5.1	2.2	42%
Liver	546	Mean	6.7	1.7	26%
Parotid	540	Mean	11.1	3.3	30%
Spleen	546	Median	6.9	3.1	46%
Sub-mandibular	543	Mean	12.1	3.4	28%
B. SUV_{peak} physiological activity					
Organ	n	Statistic	SUV_{peak}	SD/IQR	CoV
Aorta	546	Mean	2.0	0.5	22%
Bladder	546	Median	16.0	18.5	116%
Duodenum	546	Mean	11.1	3.8	34%
Gluteal	546	Mean	0.6	0.1	21%
Kidney	546	Mean	37.8	9.0	24%
Lacrimals	360	Mean	6.7	2.5	37%
Liver	546	Mean	8.2	2.1	26%
Parotid	540	Mean	16.8	5.1	30%
Spleen	546	Median	9.9	4.6	47%
Sub-mandibular	543	Mean	17.8	5.0	28%

Standard deviation is presented for normally distributed metrics while interquartile range is presented for non-normally distributed metrics. CoV, Coefficient of variation; IQR, interquartile range; SD, standard deviation.

In the key organs of liver and bladder, the SUV_{mean} in the liver was a mean of 6.7 (SD 1.7), CoV 26%; and in the bladder a median of 10.6 (IQR 11.9), CoV 112%. In the same key organs, SUV_{peak} in the liver was a mean of 8.2 (SD 2.1), CoV 26%; and in the bladder a median of 16.0 (IQR 18.5), CoV 116%.

The population distribution of SUV_{mean} and SUV_{peak} values across the key organs of interest is displayed graphically in **Figure 4**.

Discussion

^{18}F-Flotufolastat is a newly FDA-approved PSMA-targeted PET radiopharmaceutical for diagnostic imaging in patients with prostate cancer. Further to their role in diagnostic imaging, PSMA-targeted PET radiopharmaceuticals are now being utilized to help select patients with mCRPC who may benefit from PSMA-targeted RLT based on the presence of uptake in metastatic lesions greater than normal liver on PET images. This clinical use is supported by data from the Vision Trial and recommendations by the NCCN and SNMMI AUC Working Group [2, 14, 16, 20], though until now there has been limited information published around ^{18}F-flotufolastat normal organ biodistribution. We quantitatively evaluated ^{18}F-flotufolastat uptake in the liver and other normal organs to further describe its physiologic biodistribution and better inform clinicians around its use in evaluating patients who may be eligible for RLT.

This post hoc quantitative analysis of ^{18}F-flotufolastat uptake in normal organs in 718 men who underwent PET/CT in two phase 3 clinical studies shows the range of normal organs with physiological ^{18}F-flotufolastat activity to be consistent with previously published phase 1 data,[12] as well as more broadly with other PSMA radiopharmaceuticals that are predominantly excreted via the urinary tract [17, 18, 22, 23]. The highest SUV metric, mean SUV_{mean} 22.4 (SD 5.5) (mean SUV_{peak} 37.8 (SD 9.0)) was seen in the kidney, which is typical for a PSMA radiopharmaceutical. However, bladder activity median SUV_{mean} was 10.6 (IQR 11.9) (median SUV_{peak} 16.0 (IQR 18.5)); this SUV_{peak} is lower than that reported for either ^{68}Ga-PSMA-11 or ^{18}F-DCFPyL by Ferreira *et al* (43.1 and 57.3, respectively) [18], offering further support to the early clinical data, and data previously reported from this population, that show ^{18}F-flotufolastat has low average urinary excretion compared with values reported for other renally-cleared PSMA-PET radiopharmaceuticals [11, 12]. The radiohybrid technology platform from which ^{18}F-flotufolastat is developed supports optimal kidney clearance through high PSMA-binding affinity, high internalization by PSMA-expressing cells, medium-to-low lipophilicity, and high human serum albumin binding [7, 9, 24, 25]. This likely contributes to the lower average urinary activity observed for ^{18}F-flotufolastat at the time of PET imaging as illustrated by the patient image in **Figure 1**. A visual inspection of the population distribution (**Figure 4**) shows that while many subjects have low bladder SUV metrics (SUV_{mean} < circa 20, SUV_{peak} < circa 25), there are a smaller number of higher values and a few extremely high outliers which likely affected the CoV reported here. Nevertheless, as previously reported, qualitative image assessment of over 700 ^{18}F-flotufolastat PET/CT images by three blinded nuclear medicine physicians show that ^{18}F-flotufolastat urinary activity does not impact disease assessment for the vast majority (96%) of patients [11].

To date, ^{18}F-flotufolastat has been shown to offer clinically useful information regarding identification of both N1 and M1 disease prior to surgery in patients newly diagnosed with unfavourable intermediate-to-very high-risk prostate cancer [8]. In patients with biochemical recurrence, studies in the literature show ^{18}F-flotufolastat to compare favorably with the other FDA-approved PSMA-targeted PET radiopharmaceuticals, offering high patient-level detection rates in the range of 73-83% [9, 26]. Moreover, among 121 patients with very low PSA levels (<0.5 ng/mL), ^{18}F-flotufolastat has a detection rate of 64% [10], while DCFPyL and ^{68}Ga-PSMA-11 are reported to have rates of 36% and 38%, respectively [27, 28]. When comparing patient-level positive predictive values for histo-

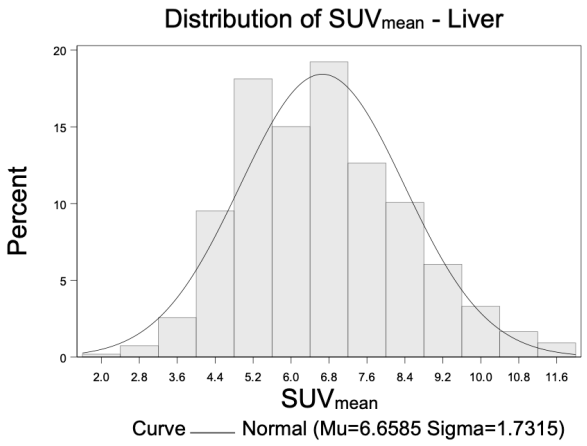
Distribution of SUVmean - Liver
Percent
SUVmean
Curve —— Normal (Mu=6.6585 Sigma=1.7315)

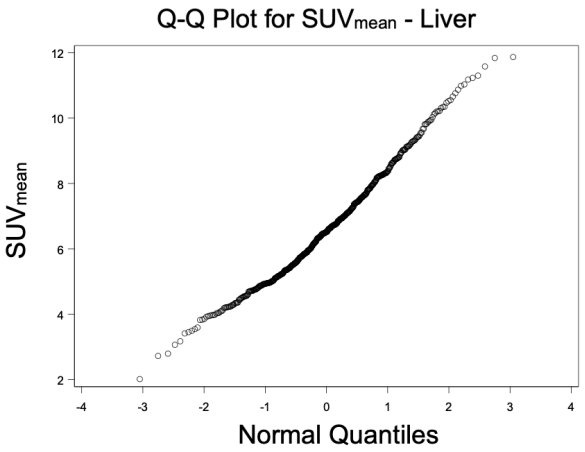
Q-Q Plot for SUVmean - Liver
SUVmean
Normal Quantiles

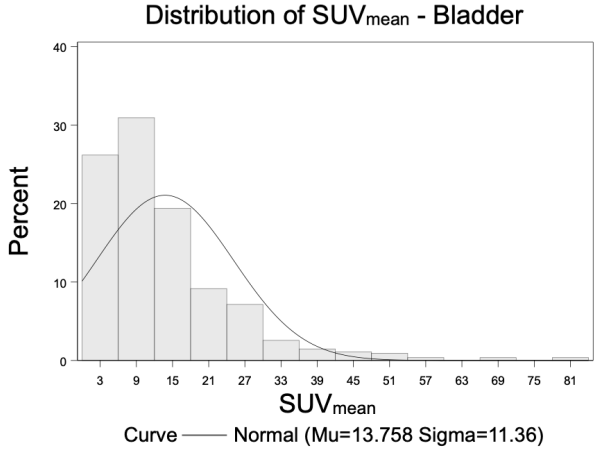
Distribution of SUVmean - Bladder
Percent
SUVmean
Curve —— Normal (Mu=13.758 Sigma=11.36)

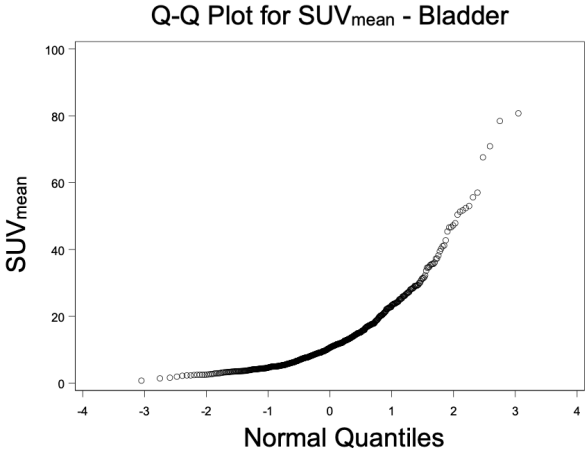
Q-Q Plot for SUVmean - Bladder
SUVmean
Normal Quantiles

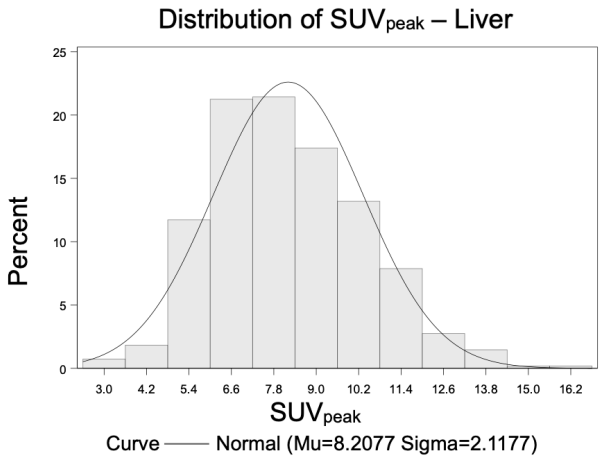
Distribution of SUVpeak – Liver
Percent
SUVpeak
Curve —— Normal (Mu=8.2077 Sigma=2.1177)

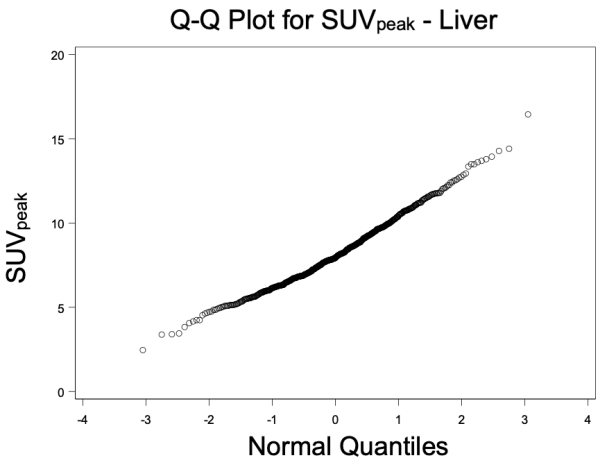
Q-Q Plot for SUVpeak - Liver
SUVpeak
Normal Quantiles

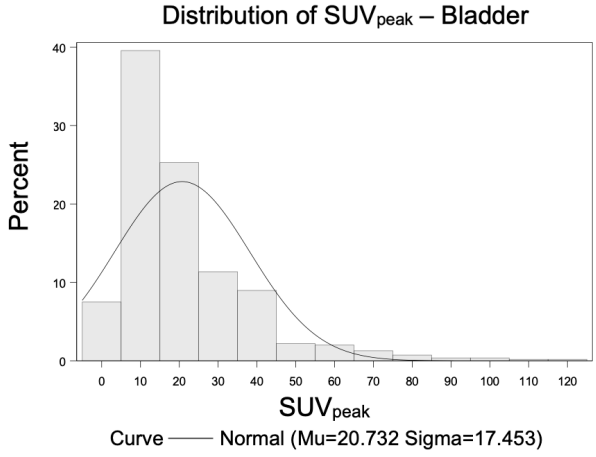
Distribution of SUVpeak – Bladder
Percent
SUVpeak
Curve —— Normal (Mu=20.732 Sigma=17.453)

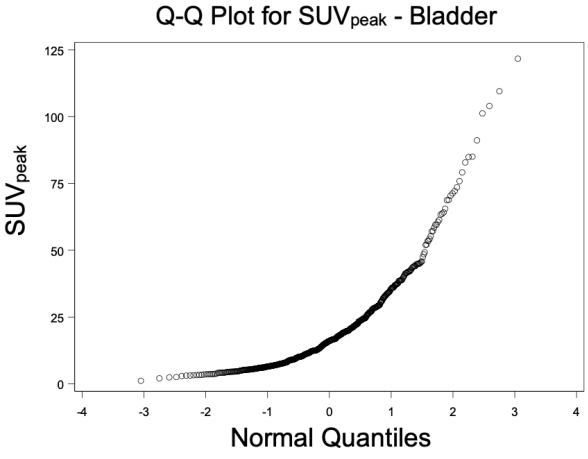
Q-Q Plot for SUVpeak - Bladder
SUVpeak
Normal Quantiles

Figure 3. Histogram and Q-Q plots of ^{18}F-flotufolastat SUV_{mean} and SUV_{peak} in the liver and bladder.

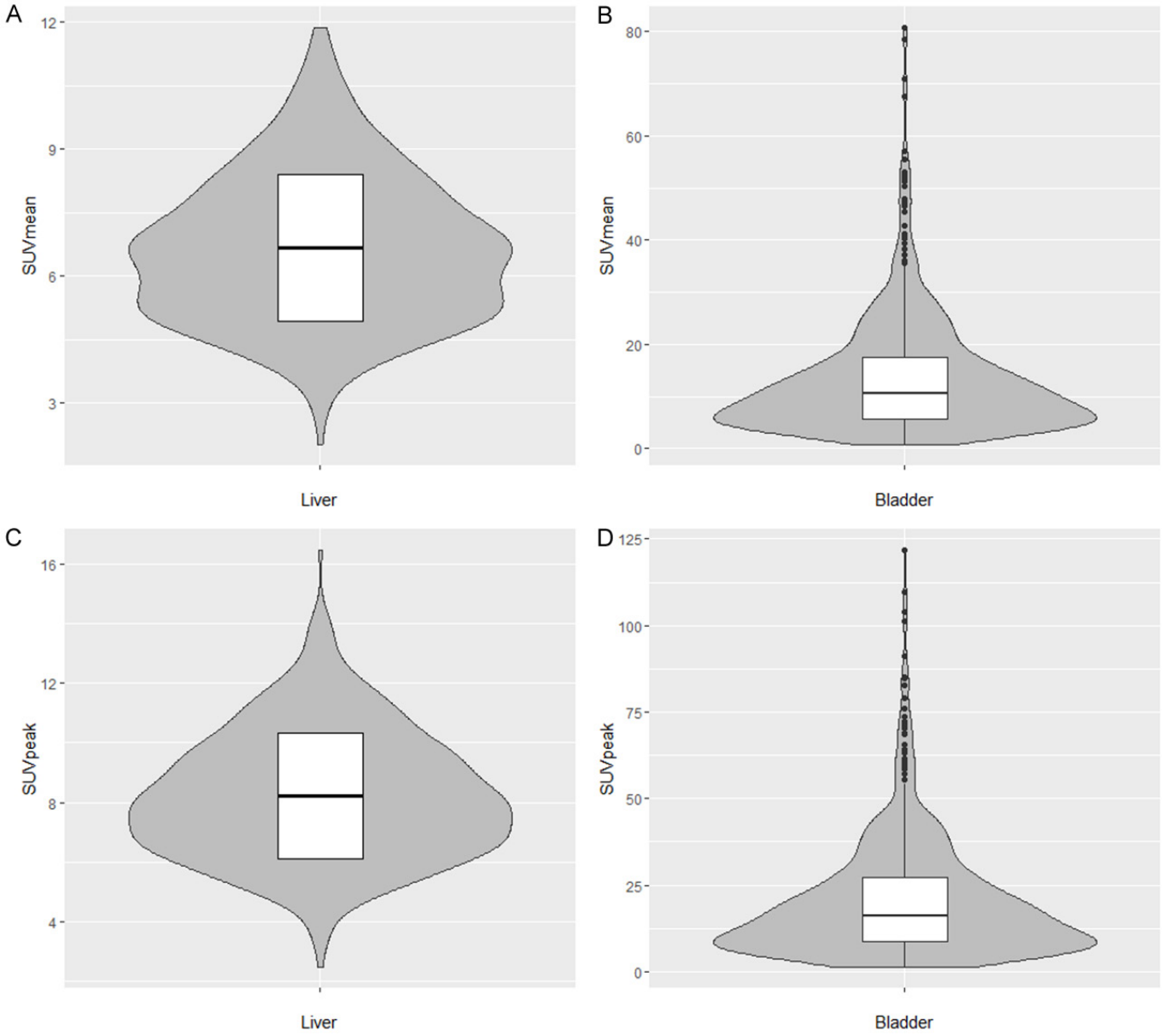

Figure 4. Box-whisker and Violin plots of SUV_{mean} (A and B) and SUV_{peak} (C and D) in the key organs of liver and bladder. Data that are non-normally distributed (B and D) are represented by median SUV metric, interquartile range, and outliers. Data that are considered normally distributed (A and C) are represented by mean SUV metric and standard deviation.

pathologically-verified lesions, all of the FDA-approved PSMA-targeting radiopharmaceuticals show similar values: 84% for ^{68}Ga-PSMA-11 [28], 79-83% for ^{18}F-DCFPyL [27], and 82% for ^{18}F-flotufolastat [9].

Further to this established favorable diagnostic performance, we show here that the range of organs with physiological ^{18}F-flotufolastat uptake is consistent with early phase data [12], and the population median SUV metric point estimates are broadly consistent with other predominantly renally-cleared PSMA-targeted radiopharmaceuticals, but with lower median bladder values as discussed above [18].

The comparison of lesion uptake with reference organs (e.g., the liver) has been successfully used with other radiopharmaceuticals and in other cancers [29]. This approach is now playing a role in RLT selection, having been used in several recent large clinical studies leading to its inclusion in the ^{68}Ga-PSMA-11 prescribing information [5, 16, 30], as well as being recommended by joint European Association of Nuclear Medicine (EANM)/SNMMI prostate cancer guidance [13]. The mean liver SUV_{peak} seen in the present study, 8.2 (SD 2.1), CoV 26%, is comparable to values reported for ^{68}Ga-PSMA-11 and ^{18}F-DCFPyL by Ferreira *et al* (6.7 (SD 1.5), CoV 21.9%, and 7.5 (SD 1.7), CoV 22.5%, respectively), further supporting

their conclusion of its suitability for use as a reference physiological organ [18]. Moreover, given the mean liver SUV_{peak} for ^{18}F-flotufolastat is comparable to values reported for ^{68}Ga-PSMA-11 and ^{18}F-DCFPyL [18], these data support using the liver as a reference physiological organ for PSMA-positive lesion identification with ^{18}F-flotufolastat, per existing practice guidance recommendations around RLT patient selection [2].

The large number of patients included in this analysis is a particular strength, allowing a robust set of data, however there are some limitations of note. While the assessment methodology in Ferreira *et al* [18] was followed as closely as possible, there are methodological differences in the data acquisition and patient populations. The data presented here are not an intra-patient comparison, and there will be variation on a per-patient basis. Additionally, there are likely differences in the hydration status of the patients evaluated in this post hoc analysis, as this was not prospectively controlled for in the original studies. Finally, this work is not intended to draw conclusions on the diagnostic efficacy of any particular PSMA radiopharmaceutical, for which a formal head-to-head study would be required.

In conclusion, these data from a large post hoc analysis show ^{18}F-flotufolastat to have comparable biodistribution to both ^{68}Ga-PSMA-11 and ^{18}F-DCFPyL in the liver, suggesting that these radiopharmaceuticals can be used interchangeably in local site protocols for evaluating patients with prostate cancer who may be eligible for RLT. Although not a head-to-head study, the newly measured ^{18}F-flotufolastat SUV_{peak} in the bladder appears lower than the reported values for other renally cleared PSMA agents.

Acknowledgements

Editorial support was provided by Dr. C Turnbull, Blue Earth Diagnostics Ltd., Oxford, UK. The LIGHTHOUSE and SPOTLIGHT studies were funded by Blue Earth Diagnostics Ltd., Oxford, UK.

Disclosure of conflict of interest

RP and JS are employees of Blue Earth Diagnostics Ltd., Oxford, UK. BF is an employee of Blue Earth Therapeutics Ltd., Oxford, UK. PD is an employee of Blue Earth Diagnostics Inc., Monroe Township, New Jersey, USA.

Address correspondence to: Ross Penny, Blue Earth Diagnostics Ltd., The Oxford Science Park, Magdalen Centre, Robert Robinson Avenue, Oxford, OX4 4GA, UK. Tel: +44-7825-924-454; E-mail: Ross.Penny@blueearthdx.com

References

[1] FDA. FDA approves first PSMA-targeted PET imaging drug for men with prostate cancer: https://www.fda.gov/news-events/press-announcements/fda-approves-first-psma-targeted-pet-imaging-drug-men-prostate-cancer. 2020.

[2] NCCN. NCCN clinical practice guidelines in oncology: prostate cancer. Version 3.2024. https://www.nccn.org/professionals/physician_gls/pdf/prostate.pdf. 2024.

[3] Cornford P, van den Bergh RCN, Briers E, Van den Broeck T, Brunckhorst O, Darraugh J, Eberli D, De Meerleer G, De Santis M, Farolfi A, Gandaglia G, Gillessen S, Grivas N, Henry AM, Lardas M, van Leenders GJLH, Liew M, Linares Espinos E, Oldenburg J, van Oort IM, Oprea-Lager DE, Ploussard G, Roberts MJ, Rouvière O, Schoots IG, Schouten N, Smith EJ, Stranne J, Wiegel T, Willemse PM and Tilki D. EAU-EANM-ESTRO-ESUR-ISUP-SIOG Guidelines on Prostate Cancer-2024 Update. Part I: screening, diagnosis, and local treatment with curative intent. Eur Urol 2024; 86: 148-163.

[4] FDA. Highlights of prescribing information: PYLARIFY® (piflufolastat F 18) injection. https://www.accessdata.fda.gov/drugsatfda_docs/label/2021/214793s000lbl.pdf, 2021.

[5] FDA. Highlights of prescribing information: Gallium Ga 68 PSMA-11 Injection. https://www.accessdata.fda.gov/drugsatfda_docs/label/2020/212642s000lbl.pdf, 2020.

[6] FDA. Highlights of prescribing information: POSLUMA (flotufolastat F 18) injection. https://www.accessdata.fda.gov/drugsatfda_docs/label/2023/216023s000lbl.pdf, 2023.

[7] Wurzer A, Di Carlo D, Schmidt A, Beck R, Eiber M, Schwaiger M and Wester HJ. Radiohybrid ligands: a novel tracer concept exemplified by ^{18}F- or ^{68}Ga-labeled rhPSMA inhibitors. J Nucl Med 2020; 61: 735-742.

[8] Surasi DS, Eiber M, Maurer T, Preston MA, Helfand BT, Josephson D, Tewari AK, Somford DM, Rais-Bahrami S, Koontz BF, Bostrom PJ, Chau A, Davis P, Schuster DM and Chapin BF; LIGHTHOUSE Study Group. Diagnostic performance and safety of positron emission tomography with ^{18}F-rhPSMA-7.3 in patients with newly diagnosed unfavourable intermediate- to very-high-risk prostate cancer: results from a phase 3, prospective, multicentre study (LIGHTHOUSE). Eur Urol 2023; 84: 361-370.

[9] Jani AB, Ravizzini GC, Gartrell BA, Siegel BA, Twardowski P, Saltzstein D, Fleming MT, Chau A, Davis P, Chapin BF and Schuster DM; SPOTLIGHT Study Group. Diagnostic performance and safety of ^{18}F-rhPSMA-7.3 positron emission tomography in men with suspected prostate cancer recurrence: results from a phase 3, prospective, multicenter study (SPOTLIGHT). J Urol 2023; 210: 299-311.

[10] Lowentritt BH, Jani AB, Helfand BT, Uchio EM, Morris MA, Michalski JM, Chau A, Davis P, Chapin BF and Schuster DM. Impact of clinical factors on ^{18}F-flotufolastat detection rates in men with recurrent prostate cancer: exploratory analysis of the phase 3 SPOTLIGHT Study. Advances in Radiation Oncology 2024; 9: 101532.

[11] Kuo PH, Hermsen R, Penny R and Postema EJ. Quantitative and qualitative assessment of urinary activity of ^{18}F-flotufolastat-PET/CT in patients with prostate cancer: a post hoc analysis of the LIGHTHOUSE and SPOTLIGHT studies. Mol Imaging Biol 2024; 26: 53-60.

[12] Tolvanen T, Kalliokoski K, Malaspina S, Kuisma A, Lahdenpohja S, Postema EJ, Miller MP and Scheinin M. Safety, biodistribution, and radiation dosimetry of ^{18}F-rhPSMA-7.3 in healthy adult volunteers. J Nucl Med 2021; 62: 679-684.

[13] Fendler WP, Eiber M, Beheshti M, Bomanji J, Calais J, Ceci F, Cho SY, Fanti S, Giesel FL, Goffin K, Haberkorn U, Jacene

H, Koo PJ, Kopka K, Krause BJ, Lindenberg L, Marcus C, Mottaghy FM, Oprea-Lager DE, Osborne JR, Piert M, Rowe SP, Schoder H, Wan S, Wester HJ, Hope TA and Herrmann K. PSMA PET/CT: joint EANM procedure guideline/SNMMI procedure standard for prostate cancer imaging 2.0. Eur J Nucl Med Mol Imaging 2023; 50: 1466-1486.

[14] Hope TA and Jadvar H. Updates to appropriate use criteria for PSMA PET. J Nucl Med 2022; 63: 14N.

[15] FDA. FDA approves Pluvicto for metastatic castration-resistant prostate cancer: https://www.fda.gov/drugs/resources-information-approved-drugs/fda-approves-pluvicto-metastatic-castration-resistant-prostate-cancer. 2022.

[16] Sartor O, de Bono J, Chi KN, Fizazi K, Herrmann K, Rahbar K, Tagawa ST, Nordquist LT, Vaishampayan N, El-Haddad G, Park CH, Beer TM, Armour A, Pérez-Contreras WJ, DeSilvio M, Kpamegan E, Gericke G, Messmann RA, Morris MJ and Krause BJ; VISION Investigators. Lutetium-177-PSMA-617 for metastatic castration-resistant prostate cancer. N Engl J Med 2021; 385: 1091-1103.

[17] Szabo Z, Mena E, Rowe SP, Plyku D, Nidal R, Eisenberger MA, Antonarakis ES, Fan H, Dannals RF, Chen Y, Mease RC, Vranesic M, Bhatnagar A, Sgouros G, Cho SY and Pomper MG. Initial evaluation of [^{18}F]DCFPyL for prostate-specific membrane antigen (PSMA)-targeted PET imaging of prostate cancer. Mol Imaging Biol 2015; 17: 565-574.

[18] Ferreira G, Iravani A, Hofman MS and Hicks RJ. Intra-individual comparison of ^{68}Ga-PSMA-11 and ^{18}F-DCFPyL normal-organ biodistribution. Cancer Imaging 2019; 19: 23.

[19] Heilinger J, Weindler J, Roth KS, Krapf P, Schomacker K, Dietlein M, Drzezga A and Kobe C. Threshold for defining PSMA-positivity prior to ^{177}Lu-PSMA therapy: a comparison of [^{68}Ga]Ga-PSMA-11 and [^{18}F]F-DCFPyL in metastatic prostate cancer. EJNMMI Res 2023; 13: 83.

[20] Hope TA and Jadvar H. PSMA PET AUC updates: inclusion of rh-PSMA-7.3. J Nucl Med 2024; 65: 540.

[21] Wahl RL, Jacene H, Kasamon Y and Lodge MA. From RECIST to PERCIST: evolving considerations for PET response criteria in solid tumors. J Nucl Med 2009; 50 Suppl 1: 122S-150S.

[22] Afshar-Oromieh A, Malcher A, Eder M, Eisenhut M, Linhart HG, Hadaschik BA, Holland-Letz T, Giesel FL, Kratochwil C, Haufe S, Haberkorn U and Zechmann CM. PET imaging with a [^{68}Ga]gallium-labelled PSMA ligand for the diagnosis of prostate cancer: biodistribution in humans and first evaluation of tumour lesions. Eur J Nucl Med Mol Imaging 2013; 40: 486-495.

[23] Prasad V, Steffen IG, Diederichs G, Makowski MR, Wust P and Brenner W. Biodistribution of [^{68}Ga]PSMA-HBED-CC in patients with prostate cancer: characterization of uptake in normal organs and tumour lesions. Mol Imaging Biol 2016; 18: 428-436.

[24] Wurzer A, Kunert JP, Fischer S, Felber V, Beck R, Rose F, D'Alessandria C, Weber W and Wester HJ. Synthesis and preclinical evaluation of ^{177}Lu-labeled radiohybrid PSMA ligands for endoradiotherapy of prostate cancer. J Nucl Med 2022; 63: 1489-1495.

[25] Wurzer A, Parzinger M, Konrad M, Beck R, Günther T, Felber V, Färber S, Di Carlo D and Wester HJ. Preclinical comparison of four [^{18}F, ^{nat}Ga]rhPSMA-7 isomers: influence of the stereoconfiguration on pharmacokinetics. EJNMMI Res 2020; 10: 149.

[26] Rauscher I, Karimzadeh A, Schiller K, Horn T, D'Alessandria C, Franz C, Worther H, Nguyen N, Combs SE, Weber WA and Eiber M. Detection efficacy of ^{18}F-rhPSMA-7.3 PET/CT and impact on patient management in patients with biochemical recurrence of prostate cancer after radical prostatectomy and prior to potential salvage treatment. J Nucl Med 2021; 62: 1719-1726.

[27] Morris MJ, Rowe SP, Gorin MA, Saperstein L, Pouliot F, Josephson D, Wong JYC, Pantel AR, Cho SY, Gage KL, Piert M, Iagaru A, Pollard JH, Wong V, Jensen J, Lin T, Stambler N, Carroll PR and Siegel BA; CONDOR Study Group. Diagnostic performance of ^{18}F-DCFPyL-PET/CT in men with biochemically recurrent prostate cancer: Results from the CONDOR phase III, multicenter study. Clin Cancer Res 2021; 27: 3674-3682.

[28] Fendler WP, Calais J, Eiber M, Flavell RR, Mishoe A, Feng FY, Nguyen HG, Reiter RE, Rettig MB, Okamoto S, Emmett L, Zacho HD, Ilhan H, Wetter A, Rischpler C, Schoder H, Burger IA, Gartmann J, Smith R, Small EJ, Slavik R, Carroll PR, Herrmann K, Czernin J and Hope TA. Assessment of ^{68}Ga-PSMA-11 PET accuracy in localizing recurrent prostate cancer: a prospective single-arm clinical trial. JAMA Oncol 2019; 5: 856-863.

[29] Barrington SF, Mikhaeel NG, Kostakoglu L, Meignan M, Hutchings M, Mueller SP, Schwartz LH, Zucca E, Fisher RI, Trotman J, Hoekstra OS, Hicks RJ, O'Doherty MJ, Hustinx R, Biggi A and Cheson BD. Role of imaging in the staging and response assessment of lymphoma: consensus of the International Conference on Malignant Lymphomas Imaging Working Group. J Clin Oncol 2014; 32: 3048-3058.

[30] Hofman MS, Violet J, Hicks RJ, Ferdinandus J, Thang SP, Akhurst T, Iravani A, Kong G, Ravi Kumar A, Murphy DG, Eu P, Jackson P, Scalzo M, Williams SG and Sandhu S. [^{177}Lu]-PSMA-617 radionuclide treatment in patients with metastatic castration-resistant prostate cancer (LuPSMA trial): a single-centre, single-arm, phase 2 study. Lancet Oncol 2018; 19: 825-833.